Multimode-pumped Raman amplification of a higher order mode in a large mode area fiber

SHENG ZHU[1], SHANKAR PIDISHETY[1,2], YUTONG FENG[1], SOONKI HONG[1], JEFF DEMAS[3,4], RAGHURAMAN SIDHARTHAN[5], SEONGWOO YOO[5], SIDDHARTH RAMACHANDRAN[3], BALAJI SRINIVASAN[2], AND JOHAN NILSSON[1*]

[1]*Optoelectronics Research Centre, University of Southampton, Southampton, SO17 1BJ, United Kingdom*
[2]*Department of Electrical Engineering, Indian Institute of Technology Madras, Chennai-600036, India*
[3]*Department of Electrical Engineering, Boston University, 8 St. Mary's St., Boston, MA 02215, USA*
[4]*Currently with the Laboratory of Neurotechnology and Biophysics, The Rockefeller University, 1230 York Ave., New York, NY 10065, USA*
[5]*School of Electrical and Electronics Engineering, Centre of Optical Fibre Technology, The Photonics Institute, Nanyang Technological University, 50 Nanyang Avenue, 639798, Singapore*
**jn@orc.soton.ac.uk*

Abstract: We report the first demonstration of Raman amplification in a fiber of a single Bessel-like higher order mode using a multimode pump source. We amplify the LP_{08}-mode with a 559-μm^2 effective mode area at a signal wavelength of 1115 nm in a pure-silica-core step-index fiber. A maximum of 18 dB average power gain is achieved in a 9-m long gain fiber, with output pulse energy of 115 μJ. The Raman pump source comprises a pulsed 1060 nm ytterbium-doped fiber amplifier with V-value ~30, which is matched to the Raman gain fiber. The pump depletion as averaged over the signal pulses reaches 36.7%. The conversion of power from the multimode pump into the signal mode demonstrates the potential for efficient brightness enhancement with low amplification-induced signal mode purity degradation.

OCIS codes: (060.2320) Fiber optics amplifiers and oscillators, (060.4370) Nonlinear optics, fibers

References and links

1. D. J. Richardson, J. Nilsson, and W. A. Clarkson, "High power fiber lasers: current status and future perspectives [Invited]," J. Opt. Soc. Am. B **27**, B63 (2010).
2. Y. Jeong, J. K. Sahu, D. N. Payne, and J. Nilsson, "Ytterbium-doped large-core fiber laser with 1.36 kW continuous-wave output power," Opt. Express **12**, 6088 (2004).
3. R. F. Cregan, "Single-Mode Photonic Band Gap Guidance of Light in Air," Science (80). **285**, 1537–1539 (1999).
4. Liang Dong, H. A. Mckay, A. Marcinkevicius, Libin Fu, Jun Li, B. K. Thomas, and M. E. Fermann, "Extending Effective Area of Fundamental Mode in Optical Fibers," J. Lightwave Technol. **27**, 1565–1570 (2009).
5. D. Jain, Y. Jung, M. Nunez-Velazquez, and J. K. Sahu, "Extending single mode performance of all-solid large-mode-area single trench fiber," Opt. Express **22**, 31078 (2014).
6. D. Jain, Novel Optical Fibers for High Power Lasers, PhD Thesis, University of Southampton (2015).
7. L. Rishøj, M. Jones, J. Demas, P. Gregg, G. Prabhakar, L. Yan, T. Hawkins, J. Ballato, and S. Ramachandran, "Polymer-clad silica fibers for tailoring modal area and dispersion," Opt. Lett. **41**, 3587 (2016).
8. S. Ramachandran, J. W. Nicholson, S. Ghalmi, M. F. Yan, P. Wisk, E. Monberg, and F. V Dimarcello, "Light propagation with ultralarge modal areas in optical fibers," Opt. Lett. **31**, 1797–1799 (2006).
9. J. M. Fini and S. Ramachandran, "Natural bend-distortion immunity of higher-order-mode large-mode-area fibers," Opt. Lett. **32**, 748 (2007).
10. S. Ramachandran, "Dispersion-tailored few-mode fibers: a versatile platform for in-fiber photonic devices," J. Lightwave Technol. **23**, 3426–3443 (2005).
11. S. Pidishety, S. Pachava, P. Gregg, S. Ramachandran, G. Brambilla, and B. Srinivasan, "Orbital angular momentum beam excitation using an all-fiber weakly fused mode selective coupler," Opt. Lett. **42**, 4347 (2017).
12. R. M. Herman and T. A. Wiggins, "Production and uses of diffractionless beams," J. Opt. Soc. Am. A **8**,

932 (1991).
13. J. Demas, L. Rishøj, and S. Ramachandran, "Free-space beam shaping for precise control and conversion of modes in optical fiber," Opt. Express **23**, 28531 (2015).
14. J. W. Nicholson, J. M. Fini, A. DeSantolo, P. S. Westbrook, R. S. Windeler, T. Kremp, C. Headley, and D. J. DiGiovanni, "A higher-order mode fiber amplifier with an axicon for output mode conversion," in *Proc. SPIE*, L. B. Shaw, ed. (2015), Vol. 9344, p. 93441V.
15. S. Ramachandran, K. Brar, S. Ghalmi, K. Aiso, M. Yan, D. Trevor, J. Fleming, C. Headley, and P. Wisk, "High-power amplification in a 2040-μm^2 higher order mode," in *SPIE Photonics West* (2007), pp. 3–4.
16. J. W. Nicholson, J. M. Fini, A. M. DeSantolo, E. Monberg, F. DiMarcello, J. Fleming, C. Headley, D. J. DiGiovanni, S. Ghalmi, and S. Ramachandran, "A higher-order-mode Erbium-doped-fiber amplifier," Opt. Express **18**, 17651 (2010).
17. R. Ryf, M. Esmaeelpour, N. K. Fontaine, H. Chen, A. H. Gnauck, R.-J. Essiambre, J. Toulouse, Y. Sun, and R. Lingle, "Distributed Raman amplification based transmission over 1050-km few-mode fiber," in *2015 European Conference on Optical Communication (ECOC)* (IEEE, 2015), pp. 1–3.
18. J. Li, J. Du, L. Ma, M. Li, K. Xu, and Z. He, "Second-order few-mode Raman amplifier for mode-division multiplexed optical communication systems," Opt. Express **25**, 810 (2017).
19. J. Ji, C. A. Codemard, M. Ibsen, J. K. Sahu, and J. Nilsson, "Analysis of the conversion to the first Stokes in cladding-pumped fiber Raman amplifiers," IEEE J. Sel. Top. Quantum Electron. **15**, 129–139 (2009).
20. J. Ji, C. A. Codemard, J. K. Sahu, and J. Nilsson, "Design, performance, and limitations of fibers for cladding-pumped Raman lasers," Opt. Fiber Technol. **16**, 428–441 (2010).
21. C. A. Codemard, J. K. Sahu, and J. Nilsson, "Tandem cladding-pumping for control of excess gain in ytterbium-doped fiber amplifiers," IEEE J. Quantum Electron. **46**, 1860–1869 (2010).
22. G. Agrawal, *Nonlinear Fiber Optics* (Elsevier, 2006), Chap. 2.
23. S. Zhu, S. Pidishety, Y. Feng, J. Demas, S. Ramachandran, B. Srinivasan, and J. Nilsson, "Multimode Raman pumping for power-scaling of large area higher order modes in fiber amplifiers," in *Laser Congr. 2017 (ASSL, LAC)* ATh4A.4.
24. C. R. Giles and E. Desurvire, "Modeling erbium-doped fiber amplifiers," J. Lightwave Technol. **9**, 271–283 (1991).
25. RP Photonics, "Fiber-Optic Simulation and Design Software RP Fiber Power," https://www.rp-photonics.com/fiberpower.html.
26. F. Capasso and P. Di Porto, "Coupled-mode theory of Raman amplification in lossless optical fibers," J. Appl. Phys. **47**, 1472–1476 (1976).
27. C. A. Codemard, High-Power Cladding-Pumped Raman and Erbium-Ytterbium Doped Fibre Sources, PhD Thesis, University of Southampton (2007).
28. R. Stolen and J. Bjorkholm, "Parametric amplification and frequency conversion in optical fibers," IEEE J. Quantum Electron. **18**, 1062–1072 (1982).
29. R. Stolen and E. P. Ippen, "Raman gain in glass optical waveguides," Appl. Phys. Lett. **22**, 276–278 (1973).

1. Introduction

Fibers with large mode area (LMA) are widely used to suppress nonlinearities in single-mode high power lasers [1]. These typically operate on the fundamental mode. As the mode area increases, several approaches have been demonstrated to maintain fundamental mode operation, including step-index fibers with ultra-low core numerical aperture (NA) [2], microstructured fibers such as photonic crystal fibers (PCFs) [3], leakage channel fibers [4], and other fibers with special refractive index profiles like trench fibers [5]. Usually, however, these fibers require sophisticated design and fabrication and the fundamental mode is susceptible to bend-induced mode area reduction [6].

Alternatively, the single mode can be a higher-order mode (HOM) rather than the fundamental mode. Generally, almost any step-index multimode fiber supports stable HOM-propagation [7]. Notably, *LP*-modes LP_{0m} with $m \geq 4$, offer significant mode area scalability and are known to display better immunity to mode coupling and bend-induced mode distortions than the fundamental mode [8,9]. As the radial modal order m increases, the effective-index difference between the desired LP_{0m} and the neighboring antisymmetric mode LP_{1m} increases, which suppresses mode coupling [8]. A HOM can be converted from the fundamental mode either in fiber by a long period grating [10] or a fiber coupler [11], or in free space with an axicon [12] or a spatial light modulator [13]. For power-scaling, the HOMs can then be amplified in LMA fibers and, optionally, converted back to the fundamental mode for diffraction-limited high power applications [14].

Rare-earth (RE) doped fiber amplifiers for HOMs, including LP_{0m}-modes, have been demonstrated, both with cladding-pumping and core-pumping [15,16]. Both with cladding-pumping and core-pumping, it is possible to pump with multimode diode lasers, which allow for high-power operation as well as brightness enhancement, where the amplified signal is brighter than both the input signal and the pump. Alternatively, it is also possible to use a fiber Raman amplifier. Compared to RE-doped fiber amplifiers, these offer well-known attractions such as wavelength agility and simpler and cheaper fiber fabrication with better control of the refractive index.

Although FRAs have also been used for HOMs [17,18], to the best of our knowledge they have not been used for LP_{0m}-modes with $m \geq 4$, nor for brightness enhancement or power scaling of such modes with high-power multimode pump sources. Still, we believe this approach offers important additional attractions for high-power single-mode FRAs. For example, cladding-pumped FRAs are prone to Raman conversion to higher Stokes orders, which limits the area ratio between the pump and signal beam to ~ 8 for efficient conversion to the 1st Stokes order [19]. Because the core must remain relatively small to support a stable fundamental mode, this limits the degree of brightness enhancement one can achieve with these designs. Furthermore, with an area ratio of 8, high efficiency is only possible for a narrow range of instantaneous power [20]. This is problematic, especially for pulses with their varying instantaneous power. However, the useful instantaneous power range can be extended by reducing the area ratio. A HOM in an amplifier core-pumped by a multimode source offers a low ratio between the areas of the pump (i.e., core) and the signal mode (~3.4 in our case) and still allows for brightness enhancement, which makes HOMs attractive for single-mode FRAs.

At the same time, a FRA is attractive for HOM amplification, since a FRA may preserve the preferred HOM better than a RE-doped fiber amplifier does thanks to not only better control of fiber perturbations, but also to the absence of local gain saturation. In RE-doped fiber amplifiers, the population inversion is depleted in regions where the signal intensity is high, which results in higher gain for the parasitic modes than for the signal mode, and hence degradation in mode purity. Such mode-selective gain saturation can be more severe in fiber amplifiers cladding-pumped by a multimode laser source, owing to strong saturation and high unsaturated gain [21]. In a FRA, the local gain does not depend on the local signal intensity, and therefore there is no local mode-selective gain saturation. There can still be non-local gain saturation arising from mode-selective pump depletion when pump power is converted to signal power during the propagation through the fiber, but this is not significant until the transverse pump distribution is altered significantly and may still only be weakly mode-selective.

In this work, we demonstrate fiber Raman amplification of pulses at 1115 nm with 8-nm linewidth in the LP_{08}-mode of a 50-µm diameter, 0.22-NA pure-silica core (index step 0.016, V = 31 at 1115 nm) in a 9-m-long fiber (FG050LGA, Thorlabs). The effective mode area of LP_{08}, calculated by $A_{eff} = \left(\iint_{-\infty}^{+\infty} |F(x,y)|^2 \, dxdy \right)^2 \Big/ \iint_{-\infty}^{+\infty} |F(x,y)|^4 \, dxdy$, where $F(x,y)$ is the transverse modal distribution of LP_{08} [22], is 559 µm^2 at 1115 nm in this fiber. A multimode Yb-doped fiber amplifier (YDFA) at 1060 nm with V-value of ~ 30 provides pulses that co-directionally pump the Raman gain fiber. The amplified signal pulses reach 115 µJ of energy and 4.6 kW of peak power with an average-power gain of 18 dB. At this gain, the pump depletion is estimated to be ~36.7%, as averaged over the signal output pulse. According to simulations, saturation-induced mode purity degradation is substantially smaller in the FRA than in the YDFA. We believe this is the first demonstration of LP_{0m} HOM fiber Raman amplification pumped by a multimode source in a configuration that allows for power-scaling and brightness enhancement. The experimental results were previously reported in ASSL [23] , but we here present a more comprehensive description and analysis.

2. Simulations and comparison of HOM degradation in YDFAs and FRAs

To investigate the difference in signal mode purity degradation arising from stimulated emission in a RE-doped fiber amplifier and stimulated Raman scattering (SRS) in a FRA, we compare how the power in LP_{08} evolves relative to the power in other modes in an YDFA and a pure-silica-core FRA with co-directional pump and signal in the continuous-wave regime. For the YDFA, we assume homogeneous broadening and use a conventional rate-equation-based model [24] as implemented in RP Fiber Power [25] to calculate the amplification of each signal mode by considering the local signal intensity and its overlap with the distribution of partly excited Yb-ions. The gain coefficient $g^w(z)$ [m^{-1}] at longitudinal coordinate z of a mode i at pump ($w = P$) or signal ($w = S$) wavelength with normalized transverse intensity distribution $\psi_i^w(r,\phi)$ is given by

$$g^w(z) = \int_0^{\infty}\int_0^{2\pi} N_0\left[\left(\sigma_e^w + \sigma_a^w\right)n_2(z,r,\phi) - \sigma_a^w\right]\psi_i^w(r,\phi)rdrd\phi \tag{1}$$

where N_0 is the total concentration of Yb-ions and σ_e^w, σ_a^w are the emission and absorption cross-sections respectively. Eq. (1) is also used to evaluate the pump evolution, for which $g^w(z) < 0$, and $\psi_i^w(r,\phi)$ may represent a suitable intensity distribution rather than an eigenmode. The fractional excitation n_2 at steady state is given by:

$$n_2 = \frac{I_P\sigma_a^P/h\nu_P + I_S\sigma_a^S/h\nu_S}{I_P(\sigma_a^P + \sigma_e^P)/h\nu_P + I_S(\sigma_a^S + \sigma_e^S)/h\nu_S + 1/\tau} \tag{2}$$

Here, $h\nu_w$ is the photon energy, I_w is the local intensity summed over all modes, and τ is the upper-state lifetime.

For the FRA, the pump power in mode i, P_i^P, and signal power in mode j, P_j^S, are determined by the following differential equations [26,27]:

$$\frac{dP_i^P(z)}{dz} = -\frac{\lambda_S}{\lambda_P}g_R\sum_{k=1}^{N_S}\frac{P_i^P(z)P_k^S(z)}{A_{i,i,k,k}^{eff}}, \tag{3}$$

$$\frac{dP_j^S(z)}{dz} = g_R\sum_{k=1}^{N_P}\frac{P_k^P(z)P_j^S(z)}{A_{j,j,k,k}^{eff}} \tag{4}$$

where g_R is the Raman gain coefficient and $A_{i,i,j,j}^{eff}$ is the effective area of the inter-modal interaction between modes i and j in the Raman process given by [28]

$$\left(A_{i,i,j,j}^{eff}\right)^{-1} = \frac{\int_0^{2\pi}\int_0^{\infty}\psi_i(r,\theta)\psi_j(r,\theta)rdrd\theta}{\int_0^{2\pi}\int_0^{\infty}\psi_i(r,\theta)rdrd\theta\int_0^{2\pi}\int_0^{\infty}\psi_j(r,\theta)rdrd\theta} \tag{5}$$

The background loss is negligible for the fiber lengths we consider.

To investigate amplification-induced mode purity degradation we launch most signal power into LP_{08} and excite all other modes with a few percent of the total signal power, as a result of imperfect launch. Several factors will affect the degradation, including initial mode purity and level of gain and gain saturation. Also, temporal and spatial coherence as well as mode coupling matter. Inherent to our approach, the mode coupling of the primary mode LP_{08} necessarily needs to be small, but since this is assumed to be particularly stable, the coupling between other signal modes may well be significant. Nevertheless, we neglect coupling between the signal modes. We also assume the signal modes to be incoherent. Indeed, they

will be coherent at the launch when they are excited from a single-mode source, but the use of a spectrally broad seed will degrade the spatial coherence between the vast majority of modes in a distance much less than 1 m. For example, with our experimental linewidth of 8.1 nm (1.95 THz), two modes with effective-index difference of 0.001 remain coherent for only ~ 15 cm. As it comes to the Raman pump, we excite the fiber modes with equal power and use the same assumption of incoherent propagation without mode coupling. Since the multimode pump source used in our experiments has a linewidth of ~ 1.8 THz, the coherence between different pump modes is quite poor. Polarization effects can further reduce the effects of coherence. We did not characterize the polarization properties, but given the linewidths and fiber lengths involved, we expect both the pump and the signal to be effectively unpolarized.

Therefore, we believe the assumption of incoherent propagation is appropriate for source linewidths exceeding ~ 30 GHz in 10 m of multimode fiber.

For the YDFA, we assume a phospho-aluminosilicate host. We consider cladding-pumping and further assume that all modes are incoherent and fully coupled so that the pump light is evenly distributed over the inner cladding. The large number of cladding-modes prevented simulations of mode-coupling-free cladding-pumping. However, simulations of mode-coupling-free core-pumping with reduced pump absorption and emission cross-sections to emulate cladding-pumping gave nearly the same result as the fully mode-coupled cladding-pumping case.

Table 1. Parameters used in the simulations

Parameter	Value for FRA	Value for YDFA
λ_P	1060 nm	975 nm
λ_S	1115 nm	1045 nm
N_0	N/A	4×10^{25} m^{-3}
Core radius	22 μm	22 μm
Core *NA*	0.20	0.20
Fiber length	10 m	10 m
P_S	320 W	2 W
P_P	32 kW	0.2 kW
g_R	45 fm/W	N/A
σ_a^P	N/A	1.650×10^{-26} m^2
σ_a^S	N/A	2.010×10^{-26} m^2
σ_e^P	N/A	1.519×10^{-26} m^2
σ_e^S	N/A	5.412×10^{-25} m^2

The parameters of the simulations are given in Table 1. These were chosen to approximately match our experiment and give an appropriate level of gain and conversion in 10 m of fiber. The core diameter and NA are the same for the FRA and YDFA, and ~ 10% smaller than those for our experiments, in order to keep the number of guided modes within limits set by the simulation software. The signal wavelength of the YDFA was chosen to match the gain peak. The choice of host and signal wavelength affects the value of the cross-sections and lifetime, and thus the saturation characteristics. The saturation characteristics are

further affected by the pump details, including pump direction. We believe our parameters lead to relatively typical saturation characteristics for an YDFA, but we have not investigated to what extent other parameter with other saturation characteristics influence the results.

The pump and signal wavelengths of the FRA were chosen to agree with experimental values, and correspond to a Raman shift of 14.0 THz (465 cm^{-1}). This differs marginally from the peak Raman shift. Therefore, the value of the Raman gain coefficient of 45 fm/W is marginally lower than the peak gain for unpolarized light in pure silica [29].

The signal seed power is 1% of the pump power. This strong seeding leads to relatively low gain, and also means that amplified spontaneous emission can be neglected. In some circumstances strong ASE can build up even if the signal gain is low, if there are regions in which the gain is not saturated, especially if the signal is not at the local gain peak [21]. However, in our case, we seed all the modes at a wavelength with gain which is everywhere at or close to the level of the local peak gain.

For the FRA, the input pump and signal power can be understood as the instantaneous powers of a pulsed device. By contrast, an YDFA is generally pumped in continuous-wave (CW) and the powers may therefore be understood as the CW power level for the pump and the average power level for the signal. Furthermore, since the rate of spontaneous-emission is in general small relative to the rate of stimulated emission, it has little impact on the gain and the saturation. These are instead primarily determined by the signal-to-pump intensity ratio.

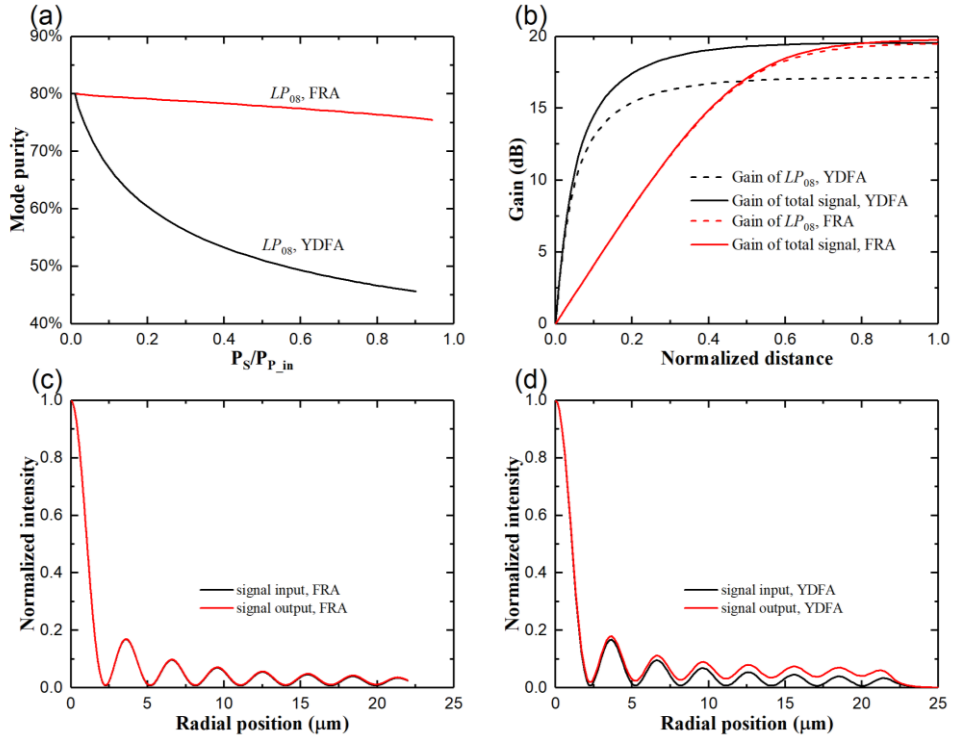

Fig. 1. (a) Evolution of LP_{08} mode purity in FRA (red curve) and YDFA (black curve) as the LP_{08}-power grows along the fiber against the signal power normalized to the launched pump power; (b) Comparison of gain in target HOM (dashed curves) and total signal (solid curves) in FRA (red curves) and YDFA (black curves); (c) Normalized transverse intensity profiles of input and output signal of FRA (curves are indistinguishable) and (d) YDFA.

Fig. 1 shows the results of our simulations when we launch 80% of the initial signal power into LP_{08} and the rest evenly into all other modes (accounting for degeneracy). We define the mode purity as the ratio of the target HOM power at signal wavelength to the total signal power. Fig. 1(a) shows the degradation of LP_{08} mode purity *vs*. the total signal power,

normalized to the launched pump power. The mode purity drops by 2.44 dB (from 80% to 45.6%) in the YDFA, but only by 0.26 dB (to 75.4%) in the FRA. Fig. 1(b) shows how the total signal power and the power in LP_{08} grow in the two amplifiers. The transverse intensity profile also degrades more in the YDFA (Fig. 1(d)) than in the FRA (Fig. 1(c)). Since there is no coupling between the signal modes in the simulations, we attribute the much larger degradation in the YDFA to mode-selective gain saturation. Although not investigated here, a core-pumped YDFA can be less affected by gain saturation [21] and may therefore preserve the purity better than a cladding-pumped YDFA.

3. Experimental setup and results

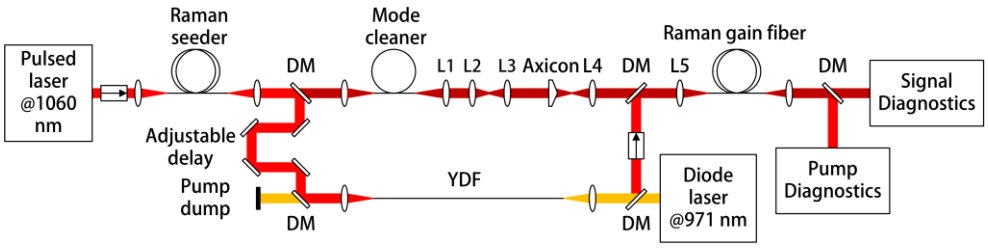

Fig. 2. Schematic of experimental setup for the fiber Raman amplification experiment consisting of the signal arm (top) and the pump arm (bottom) originating from a pulsed laser at 1060 nm.

The experimental setup of the HOM fiber Raman amplifier is shown in Fig. 2. A commercial Yb-doped fiber (YDF) laser (G3, SPI Lasers) emitting 1060-nm, 60-ns pulses at 4 kHz serves as the master oscillator. The 1060-nm pulses are partly converted into 1115-nm Stokes pulses via stimulated Raman scattering in a 30-m long Ge-doped silica fiber (Freelight, Pirelli). The output beam is split into two branches by a dichroic mirror (DM). The residual 1060-nm pulses are sent into one branch (bottom part of Fig. 2) for amplification in a 2-m long multimode YDF with core diameter of 50 µm and NA of 0.2. The fiber preform was fabricated by Nanyang Technological University through conventional modified chemical vapor deposition with chelate gas phase delivery and then drawn to a double-clad fiber with low-index coating. The YDF is cladding-pumped at 971 nm by a CW diode laser (LDL 80-500, Laserline). In the other branch (top part of Fig. 2), the 1115-nm Raman seed pulses from the Freelight fiber are propagated through a 3-m long single-mode fiber (1060-XP, Nufern) for achieving a clean fundamental LP_{01} mode. The output is then collimated by an aspheric lens (f_{L1} = 8 mm), expanded by a two-lens telescope (f_{L2} = 100 mm and f_{L3} = 250 mm) and converted to a Bessel beam by an axicon (AX251-C, Thorlabs). Another pair of lenses (f_{L4} = 250 mm and f_{L5} = 8 mm, asphere) are used to image the axicon's focal plane [13] onto the facet of the 9-m long Raman gain fiber (FG050LGA, Thorlabs) to excite the LP_{08} mode. At 1115 nm, the effective index difference between the LP_{08} mode and its nearest neighbor antisymmetric mode (LP_{18}) in the Raman gain fiber, calculated by the scalar mode solver of RP Fiber Power, is 1.252×10^{-3} in comparison to an effective index splitting of 1.452×10^{-4} between LP_{01} and LP_{11}. As mentioned in the Introduction, we expect increased stability of LP_{08} over the fundamental mode in this fiber. The 1115-nm pulses, with about 1.75 µJ energy and 60 W instantaneous power, serve as the Raman input signal and are recombined with the amplified 1060-nm pulses (pump) by another DM before being launched into the Raman gain fiber. A delay line consisting of four broadband mirrors synchronizes the pump and signal pulses. A maximum of 1.04 mJ pump energy (21.5 kW of peak power) could be launched into the Raman gain fiber. The output of the gain fiber is collimated by an aspheric lens, separated into pump and signal beam by a DM, and diagnosed by a thermal power meter, a 12.5 GHz InGaAs detector (ET-3500, EOT) connected to a 6-GHz oscilloscope (Infiniium 54855A, Agilent), an optical spectrum analyzer (OSA) (AQ6317B, Ando) and a silicon camera (BA CAM, HAAS Laser).

Fig. 3(a) shows the measured average-power gain (measured with a thermal power meter) versus launched peak pump power, estimated based on the measurement of the throughput pump power with negligible fiber loss. A maximum of 18 dB gain is achieved. The estimated pump depletion $\eta_{depletion}$ versus launched peak power is also plotted in Fig. 3(a) (right scale). It is estimated by weighting the instantaneous depletion $\eta_P(t) = \left(P_P^{in}(t) - P_P^{out}(t)\right) \Big/ P_P^{in}(t)$ with the instantaneous signal output power:

$$\eta_{depletion} = \frac{\int P_S^{out}(t)\eta_P(t)dt}{\int P_S^{out}(t)dt} \tag{6}$$

where P_P^{in}, P_P^{out}, P_S^{out} are input pump, output pump, and output signal power, respectively. At maximum gain, the average pump depletion is about 36.7%, calculated from the temporal shapes of pump and signal pulses. These are shown in Fig. 3(b) and 3(c). Fig. 3(b) also shows that the peak pump power drops by 58% and the instantaneous power at the peak at 3 ns drops by 76% (to 24%). Fig. 3(d) shows the spectra of the amplified Raman signal at various gain levels, where 0 dB gain corresponds to the input spectrum. Although the spectrum for the highest gain level of 18 dB in Fig. 3d shows an extended tail at longer wavelength, the fraction of power beyond 1130 nm is 10 dB less than the power at 1115 nm and we did not observe any significant spectral signature corresponding to the second order Raman Stokes component.

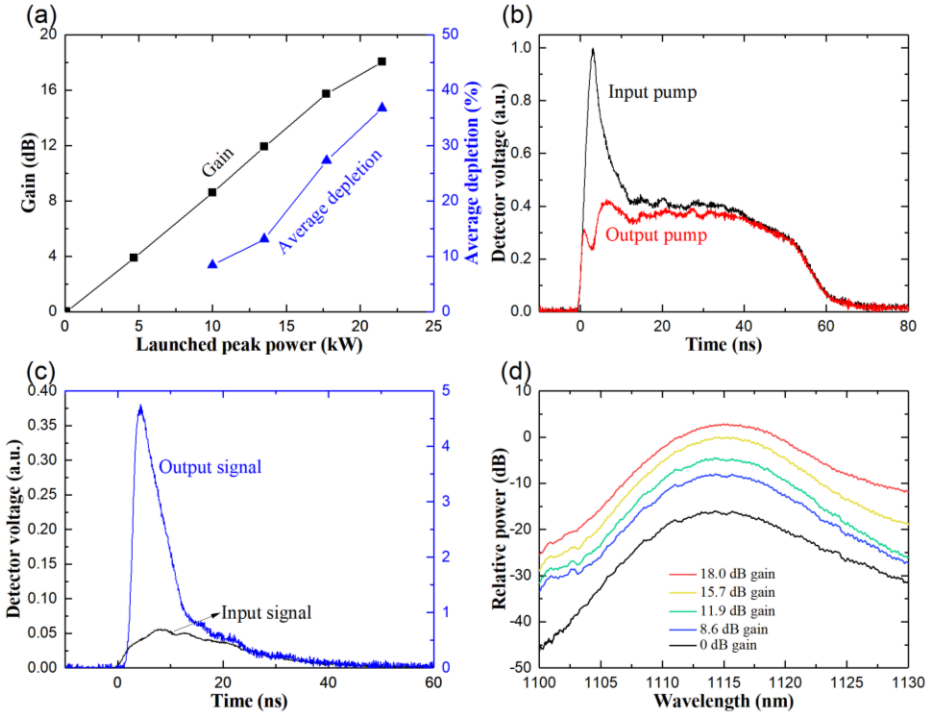

Fig. 3. (a) Measured average-power gain and average pump depletion versus launched peak pump power; (b) Pump pulse at input (black curve) and output (red curve) of Raman amplifier at 18 dB signal gain; (c) Signal pulse at input (black curve) and output (blue curve) of FRA at 16 dB gain. Note different scales for input and output signal. (d) Spectra of amplified signal measured with 0.5 nm resolution for average gain between 0 dB (bottom) and 18.0 dB (top);

The average-power gain grows almost linearly with pump peak power up to around 16 dB gain for 17.7 kW of peak power. The slope is 0.9 dB/kW, which agrees with the theoretical value with 1960 μm^2 core area and 45 fm/W Raman gain coefficient for a signal at 1115 nm

for pure silica with unpolarized pumping at 1060 nm. Beyond 17.7 kW of pump peak power, there is a slight roll-off due to pump depletion. The experimental depletion of 36.7% at highest pump power was in reasonable agreement with simulations, which showed 43.5% of depletion. Note that the peak pump power is calculated based on the pulse energy and the pulse duration over which the pump and signal overlaps. Such a calculation accounts for the large difference in the temporal shapes of the pump and signal pulses although there is still significant uncertainty in this determination.

The spatial intensity profiles of the output beams at different amplification levels are shown in Fig. 4. The ideal LP_{08}-mode comprises seven rings around a central peak, all having similar energy and separated by true nulls. The non-zero minima obtained experimentally even without pumping in Fig 4(a) and (d) indicate an imperfect signal launch, which may originate from imperfect mode-matching and misalignment. There is also some variation of the fiber modes as well as the Bessel beam generated by the axicon across the signal linewidth, but this variation is small. As the signal amplification increases up to 15.7 dB gain, shown in Fig. 4 (b) and as the red curve in Fig. 4(d), the rings near the central peak merge to some degree, but overall the purity degradation seems minor. At the maximum gain of 18 dB, (Fig. 4(c) and (d), green curve) there is further degradation. According to the simulations in Sec. 2, this degradation is not explained by mode-selective gain saturation. Instead, we suggest that the thermal load at the fiber input may have deteriorated the signal launch and that this is the primary cause of the further degradation. Further investigations on this aspect are likely to clarify the causes of mode purity degradation, and may identify means to improve.

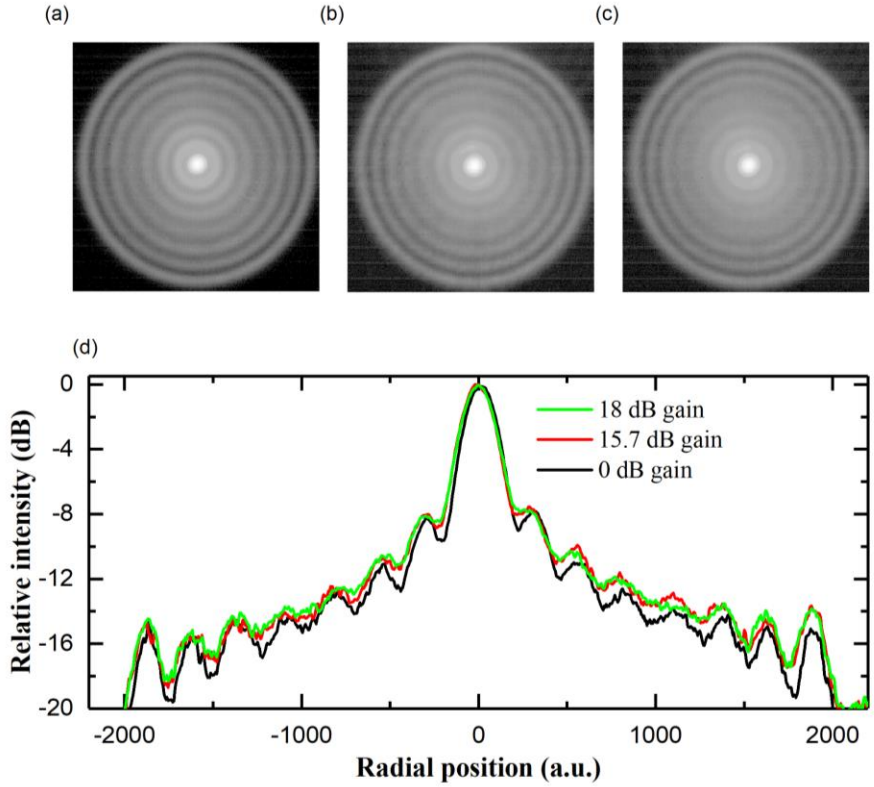

Fig. 4. Signal output beams. Images at gain levels of (a) 0 dB, (b) 15.7 dB and (c) 18 dB. The greyscale is in log scale and normalized to enhance contrast. The bright spot in the center corresponds to maximum intensity. (d) Normalized intensity line profiles (in log scale) for different gain values, 0 dB (black curve), 15.7 dB (red curve), and 18 dB (green curve). Data recorded by a silicon camera.

4. Conclusions

We have experimentally demonstrated the first fiber Raman amplifier for LP_{0m} higher order modes pumped by a multimode source. Up to 18 dB of Raman amplification of the LP_{08}-mode is achieved in a 9-m long 50-µm diameter core commercial step-index silica fiber. The HOM is excited by a free space converted Bessel beam at 1115 nm and Raman amplified by means of a 1060 nm multimode pump. The target HOM is preserved throughout the amplification with partial degradation, which we attribute primarily to imperfect excitation of the desired LP_{08} mode. With further optimized amplifier design, higher gain and pump conversion are expected, which points towards power-scaling and brightness enhancement with clean and stable HOMs in large mode area fibers of a cost-effective and mature type.

All data supporting this study are available from the University of Southampton at https://doi.org/10.5258/SOTON/D0529.

Acknowledgment

We thank Dr Rüdiger Paschotta for help with RP Fiber Power.

Funding

AFOSR (FA2386-16-1-0005, FA9550-15-1-0041, FA9550-14-1-0165); IIT Madras (YSS/2015/000713), EPSRC (Institutional Sponsorship 2016/17), ONR (N00014-17-1-2519), the Royal Academy of Engineering distinguished visitor fellowship program. S. Zhu is supported by the China Scholarship Council. S. Yoo acknowledges support from Korea Evaluation Institute of Industrial Technology.